

EFFECT OF KERR FOUNDATION AND IN-PLANE FORCES ON FREE VIBRATION OF FGM NANOBAMS WITH DIVERSE DISTRIBUTION OF POROSITY

Piotr JANKOWSKI*

*Faculty of Mechanical Engineering, Bialystok University of Technology, ul. Wiejska 45C, 15-351 Bialystok, Poland

p.jankowski@doktoranci.pb.edu.pl

Received 19 June 2020, revised 20 October 2020, accepted 23 October 2020

Abstract: In the present paper, the effect of diverse distribution of functionally graded porous material and Kerr elastic foundation on natural vibrations of nanobeams subjected to in-plane forces is investigated based on the nonlocal strain gradient theory. The displacement field of the nanobeam satisfies assumptions of Reddy higher-order shear deformation beam theory. All the displacements gradients are assumed to be small, then the components of the Green-Lagrange strain tensor are linear and infinitesimal. The constitutive relations for functionally graded (FG) porous material are expressed by nonlocal and length scale parameters and power-law variation of material parameters in conjunction with cosine functions. It created possibility to investigate an effect of functionally graded materials with diverse distribution of porosity and volume of voids on mechanics of structures in nano scale. The Hamilton's variational principle is utilized to derive governing equations of motion of the FG porous nanobeam. Analytical solution to formulated boundary value problem is obtained in closed-form by using Navier solution technique. Validation of obtained results and parametric study are presented in tabular and graphical form. Influence of axial tensile/compressive forces and three different types of porosity distribution as well as stiffness of Kerr foundation on natural frequencies of functionally graded nanobeam is comprehensively studied.

Keywords: Porosity distribution; nanobeam; Reddy beam theory; free vibrations; nonlocal strain gradient theory

1. INTRODUCTION

Recent research and development in nanotechnology have contributed to design devices in nano and micro scale called nanoelectromechanical (NEMS) and microelectromechanical (MEMS) systems (Lyshevski, 2002). NEMS and MEMS may be used in many areas including automotive, aerospace, biotechnology, healthcare, office equipment and telecommunication (Leondes, 2006). Nano and micro devices, depending on requirements, can be manufactured with porous materials (Bhushan, 2004), functionally graded materials (FGMs) (Ashoori et al., 2017) and it commonly takes the form of plates and beams (Lam et al., 2003).

To consider nano/micro size scale effect on structures nonlocal theories have been derived, for instance couple stress theory (Toupin, 1962), modified couple stress theory (Yang et al., 2002), Eringen's nonlocal theory (Eringen and Edelen, 1972; Eringen, 1972), strain gradient theory (Mindlin, 1964, 1965) and nonlocal strain gradient theory (Lim et al., 2015).

The literature survey related to the study of mechanical behavior of nanobeams is conducted to justify the originality of the present paper. The review is divided into two paragraphs: considering the effect of elastic foundation and mechanical response of nanostructures without foundation.

Aydogdu (2008) studied the influence of length to thickness ratio on bending, buckling and free vibrations based on Eringen's nonlocal theory and various beam models. Lim et al. (2010) analyzed the free vibration of axially pre-tensioned nanobeams with various boundary condition according to Eringen's nonlocal elasticity. Sahmani and Ansari (2011) presented buckling analysis with

comparison of Euler-Bernoulli, Timoshenko and Levinson beam theory with different boundary condition using Eringen's nonlocal elasticity. Thai (2012) introduced new nonlocal shear deformation beam theory and analyzed the mechanical behavior of simply supported nanobeam. Thai and Vo (2012a) investigated deflection, buckling and free vibrations of nanobeam on the basis of sinusoidal shear deformation theory and nonlocal constitutive relations of Eringen. Eltahaer et al. (2012, 2013) used finite element method to investigate free vibration and static buckling behaviors of functionally graded nanobeam based on Euler-Bernoulli model assumptions and Eringen's nonlocal theory. Nazemnezhad and Hosseini-Hashemi (2014) examined the nonlinear free vibrations of FGM Euler-Bernoulli nanobeam using Eringen's nonlocal theory. Şimşek (2014) studied the effect of aspect ratio and Eringen's nonlocal parameter on nonlinear frequency of nanobeam. Rahmani and Jandaghian (2015) conducted buckling analysis of functionally graded nanobeam using Eringen's nonlocal and Reddy beam theories. Li and Hu (2015) examined deflection and buckling of Euler-Bernoulli nanobeam model on the basic of nonlocal strain gradient theory. Şimşek (2016) employed Euler-Bernoulli beam assumptions and nonlocal strain gradient theory to study the nonlinear free vibration of simply supported nanobeam made of functionally graded material. Lu et al. (2017) developed sinusoidal shear deformation beam theory to analyze free vibration problems of simply supported nanobeam using nonlocal strain gradient theory. Shafiei et al. (2017) applied Timoshenko beam model to study the influence of porosity on vibration problems of functionally graded nano and micro beams. Eltahaer et al. (2018) presented the finite element method to study the bending and vibrations of functionally graded nanobeam with porosity according to Euler-Bernoulli beam and Eringen's nonlocal

theories. Zhang et al. (2019) investigated the influence of Eringen's nonlocal parameter, power index and length to thickness ratio on natural vibrations of functionally graded nanobeam with various boundary condition.

El-Borgi et al. (2015) considered free and forced vibration of functionally graded nanobeam resting on nonlinear elastic foundation on the basis of Euler-Bernoulli beam model assumptions and Eringen's nonlocal theory. Ghadiri et al. (2017) presented the analytical solution for nonlinear vibrations of functionally graded visco-elastically supported nanobeam subjected to transverse concentrated load. Saffari et al. (2017) studied the free vibration of simply supported FGM nanobeam resting on Winkler-Pasternak foundation based on Timoshenko beam model and Eringen's nonlocal elasticity. Reza Barati (2017) examined the forced vibrations of FGM nanobeam resting on Kerr foundation under hydro-thermal loads on the basis of sinusoidal shear deformation theory and Eringen's nonlocal theory. Lv et al. (2018) analyzed the effect of Winkler foundation and material defects on nonlinear vibrations of FGM Timoshenko nanobeam via nonlocal strain gradient theory. Karami and Janghorban (2019) proposed a new shear deformation theory and analyzed the free vibration of functionally graded nanobeam resting on Winkler-Pasternak foundation using nonlocal strain gradient theory.

The carried out literature review indicates that there does not exist an analysis of effect of stiffness of Kerr foundation and in-plane axial forces on free vibration of FGM nanobeam with diverse distributions of porosity based on the nonlocal strain gradient-based Reddy higher-order shear deformation theory. Unlike other nonlocal models, the utilized nonlocal strain gradient model is a hybrid nonlocal model, which can capture both hardening and softening phenomena in structures in nano scale. For the first time, influences of Kerr elastic foundation, volume of pores, diverse distribution of porosity and functionally graded material as well as both small scale parameters on dynamical response of nanobeams subjected to axial compressive/tensile loads were presented. Additionally, for the first time, comparison of Winkler-Pasternak and Kerr foundation effect on eigenfrequencies of simply-supported FGM nanobeam is shown.

2. DISPLACEMENT AND STRAIN FIELDS

Consider a functionally graded porous nanobeam under an axial in-plane forces \hat{N}_{xx} and resting on three-parametric foundation. Let L , h and b denote the length, thickness and width of the nanobeam, respectively. The foundation is described by springs stiffness (K_l, K_u) and shear (G) stiffness of layer. The coordinate system (x, z) and cross-section are presented in Fig. 1.

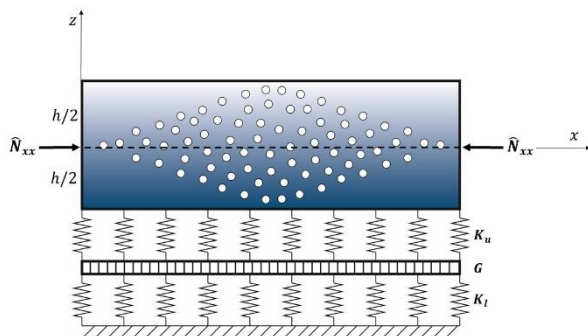


Fig. 1. The geometry and coordinate system of FGM porous nanobeam subjected to in-plane axial forces

Based on the higher-order shear deformation theory, the displacement field of the nanobeam takes the form (Reddy, 2017):

$$u_x(x, z, t) = u_0(x, t) + z\varphi_x(x, t) - c_1 z^3 \left(\varphi_x(x, t) + \frac{\partial w_0(x, t)}{\partial x} \right) \quad (1a)$$

$$u_z(x, t) = w_0(x, t) \quad (1b)$$

where u_x and u_z are displacements along x and z directions, respectively. u_0 , w_0 and φ_x are unknown generalized displacements. Hence, u_0 and w_0 denote axial and transverse displacement of a material point in the mid-plane $(x, 0)$ in the undeformed configuration at any time t . φ_x is rotation of the point on the centroidal axis x of the beam, and $c_1 = 4/(3h^2)$.

Taking into account the assumptions that all the displacement gradients are very small, consequently, the components of Green-Lagrange strain tensor are linear and infinitesimal. The general forms of strain-displacement relations associated with the displacement field (1) are defined as:

$$\varepsilon_{xx} = \varepsilon_{xx}^{(0)} + z\varepsilon_{xx}^{(1)} + z^3\varepsilon_{xx}^{(3)} \quad (2a)$$

$$2\varepsilon_{xz} = \gamma_{xz}^{(0)} + z^2\gamma_{xz}^{(2)} \quad (2b)$$

where the particular components of the linear strains are:

$$\left\{ \varepsilon_{xx}^{(0)}, \varepsilon_{xx}^{(1)}, \varepsilon_{xx}^{(3)} \right\} = \left\{ \frac{\partial u_0}{\partial x}, \frac{\partial \varphi_x}{\partial x}, -c_1 \left(\frac{\partial \varphi_x}{\partial x} + \frac{\partial^2 w_0}{\partial x^2} \right) \right\} \quad (3a)$$

$$\left\{ \gamma_{xz}^{(0)}, \gamma_{xz}^{(2)} \right\} = \left\{ \varphi_x + \frac{\partial w_0}{\partial x}, -c_2 \left(\varphi_x + \frac{\partial w_0}{\partial x} \right) \right\} \quad (3b)$$

where $c_2 = 3c_1$.

3. CONSTITUTIVE RELATIONS

On the basis of reduced higher-order nonlocal strain gradient theory (Lim et al., 2015) to only one length scale parameter, the constitutive relations of the nanobeam are expressed as:

$$(1 - \mathfrak{B}\nabla^2)\sigma_{xx} = (1 - \ell^2\nabla^2)C_{xx}\varepsilon_{xx} \quad (4a)$$

$$(1 - \mathfrak{B}\nabla^2)\sigma_{xz} = (1 - \ell^2\nabla^2)2C_{xz}\varepsilon_{xz} \quad (4b)$$

where nonlocal parameter $\mathfrak{B} = (e_0 a)^2$ describes nonlocal stress field, material length scale parameter ℓ captures higher-order strain gradient stress field, and $\nabla^2 = \frac{\partial^2}{\partial x^2}$ is the Laplace operator.

Stiffness coefficients of the FGM porous nanobeam are:

$$C_{xx} = E(z) \quad (5a)$$

$$C_{xz} = \frac{E(z)}{2(1+\nu)} \quad (5b)$$

where Poisson's ratio ν is assumed to be constant and Young's modulus $E(z)$ varies through the nanobeam thickness according to the power-law (Kim et al., 2019):

$$E(z) = \left[(E_t - E_b) \left(\frac{z}{h} + \frac{1}{2} \right)^g + E_b \right] [1 - Y(z, \vartheta)] \quad (6)$$

where E_t and E_b are Young's modulus at the top ($z = h/2$) and bottom ($z = -h/2$) surface, respectively. The constant g is power-law index and $Y(z, \vartheta)$ is a porosity distribution function. In the present paper, three different types of porosity are considered and written as:

$$\text{Type 1: } Y(z, \vartheta) = \vartheta \cos\left(\frac{\pi z}{h}\right) \quad (7a)$$

$$\text{Type 2: } Y(z, \vartheta) = \vartheta \cos\left[\frac{\pi}{2}\left(\frac{z}{h} - \frac{1}{2}\right)\right] \quad (7b)$$

$$\text{Type 3: } Y(z, \vartheta) = \vartheta \cos\left[\frac{\pi}{2}\left(\frac{z}{h} + \frac{1}{2}\right)\right] \quad (7c)$$

where ϑ is porosity coefficient. Types of porosity distribution through nanobeam thickness is presented in Fig. 2.

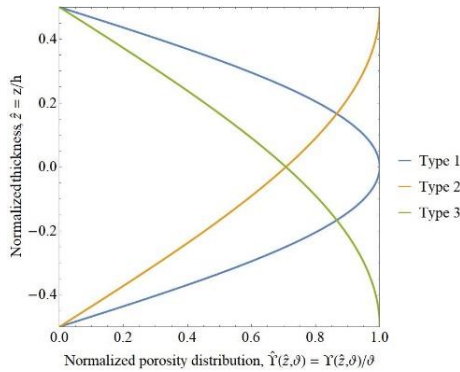


Fig. 2. Normalized distributions of porosity through nanobeam thickness

An example of effect of both power-law index and types of porosity distributions (with constant porosity coefficient value) on the variation of Young's modulus is shown in Fig. 3.

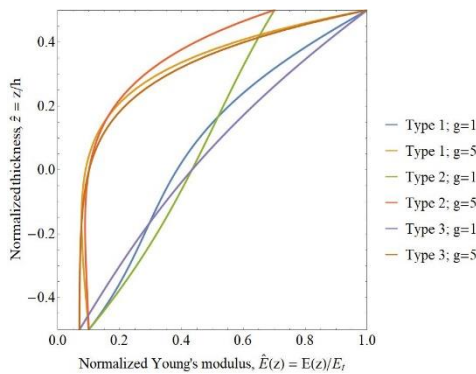


Fig. 3. Variations of Young's modulus through beam thickness depending on power-law index and porosity distribution

Substituting strains (Eq. 2) into equations (4), particular form of constitutive relations are obtained:

$$(1 - \mathfrak{B}\nabla^2)\sigma_{xx} = (1 - \ell^2\nabla^2)C_{xx}\left[\frac{\partial u_0}{\partial x} + z\frac{\partial \varphi_x}{\partial x} - c_1 z^3\left(\frac{\partial \varphi_x}{\partial x} + \frac{\partial^2 w_0}{\partial x^2}\right)\right] \quad (8a)$$

$$(1 - \mathfrak{B}\nabla^2)\sigma_{xz} = (1 - \ell^2\nabla^2)C_{xz}\left[\varphi_x + \frac{\partial w_0}{\partial x} - c_2 z^2\left(\varphi_x + \frac{\partial w_0}{\partial x}\right)\right] \quad (8b)$$

4. EQUATIONS OF MOTION

Equations of motion of the nanobeam are derived based on the dynamic version of Hamilton principle (Reddy, 2017):

$$\int_0^T (\delta U - \delta \mathcal{K} + \delta \mathcal{V}) dt = 0 \quad (9)$$

The quantities δU , $\delta \mathcal{K}$ and $\delta \mathcal{V}$ are the virtual strain energy, kinetic energy and work done by external forces, respectively. Each virtual energy and the virtual work are defined as:

$$\delta U = \int_0^L \int_A (\sigma_{xx} \delta \varepsilon_{xx} + 2\sigma_{xz} \delta \varepsilon_{xz}) dA dx \quad (10a)$$

$$\delta \mathcal{K} = \int_0^L \int_A \rho(z) (\dot{u}_x \delta \dot{u}_x + \dot{u}_z \delta \dot{u}_z) dA dx \quad (10b)$$

$$\delta \mathcal{V} = - \int_L \left[\hat{N}_{xx} \frac{\partial w_0}{\partial x} \frac{\partial \delta w_0}{\partial x} + F_f \delta w_0 \right] dz \quad (10c)$$

where $dA = b dz$, \hat{N}_{xx} are the axial in-plane compressive/tensile forces, F_f denotes a reaction of elastic foundation, and $\rho(z)$ is the mass density of the FGM porous nanobeam

$$\rho(z) = \left[(\rho_t - \rho_b) \left(\frac{z}{h} + \frac{1}{2}\right)^g + \rho_b \right] [1 - Y(z, \vartheta)] \quad (11)$$

that varies from a value at the bottom surface ρ_b to a value at the top surface ρ_t .

The particular form of the strain energy (Eq. 10a) is presented below:

$$\delta U = \int_0^L \left[N_{xx} \frac{\partial \delta u_0}{\partial x} + M_{xx} \frac{\partial \delta \varphi_x}{\partial x} - c_1 P_{xx} \left(\frac{\partial \delta \varphi_x}{\partial x} + \frac{\partial^2 \delta w_0}{\partial x^2} \right) + N_{xz} \left(\delta \varphi_x + \frac{\partial \delta w_0}{\partial x} \right) - c_2 R_{xz} \left(\delta \varphi_x + \frac{\partial \delta w_0}{\partial x} \right) \right] dx \quad (12)$$

where introduced thickness-integrated forces and moments take the following form:

$$\{N_{xx}, M_{xx}, P_{xx}\} = b \int_{-h/2}^{h/2} \sigma_{xx} \{1, z, z^3\} dz \quad (13a)$$

$$\{N_{xz}, R_{xz}\} = b \int_{-h/2}^{h/2} \sigma_{xz} \{1, z^2\} dz \quad (13b)$$

The final form of virtual kinetic energy (Eq. 10b) is expressed as:

$$\delta \mathcal{K} = \int_0^L I_0 (\dot{u}_0 \delta \dot{u}_0 + \dot{w}_0 \delta \dot{w}_0) + I_1 (\dot{u}_0 \delta \dot{\varphi}_x + \dot{\varphi}_x \delta \dot{u}_0) + I_2 (\dot{\varphi}_x \delta \dot{\varphi}_x) - c_1 I_3 \left(\dot{u}_0 \delta \dot{\varphi}_x + \dot{u}_0 \frac{\partial \delta \dot{w}_0}{\partial x} + \dot{\varphi}_x \delta \dot{u}_0 + \frac{\partial \dot{w}_0}{\partial x} \delta \dot{u}_0 \right) - c_1 I_4 \left(\dot{\varphi}_x \delta \dot{\varphi}_x + \dot{\varphi}_x \frac{\partial \delta \dot{w}_0}{\partial x} + \dot{\varphi}_x \delta \dot{\varphi}_x + \frac{\partial \dot{w}_0}{\partial x} \delta \dot{\varphi}_x \right) + c_1^2 I_6 \left(\dot{\varphi}_x \delta \dot{\varphi}_x + \dot{\varphi}_x \frac{\partial \delta \dot{w}_0}{\partial x} + \frac{\partial \dot{w}_0}{\partial x} \delta \dot{\varphi}_x + \frac{\partial \dot{w}_0}{\partial x} \frac{\partial \delta \dot{w}_0}{\partial x} \right) dx \quad (14)$$

where introduced mass inertias are defined as:

$$I_i = b \int_{-h/2}^{h/2} \rho(z) z^i dz \quad \wedge \quad i \in \{0, 6\} \quad (15)$$

The particular form of work done by external forces (Eq. 10c) takes the form:

$$\delta \mathcal{V} = - \int_L \left[-\hat{N}_{xx} \frac{\partial^2 w_0}{\partial x^2} \delta w_0 + F_f \delta w_0 \right] dz \quad (16)$$

The reaction of foundation is modeled as Kerr foundation (Kerr, 1965):

$$F_f \equiv F_k = - \left(\frac{K_l K_u}{K_l + K_u} \right) w_0 + \left(\frac{G K_u}{K_l + K_u} \right) \frac{\partial^2 w_0}{\partial x^2} \quad (17)$$

with lower K_l and upper K_u spring stiffness coefficients. G represents stiffness of shear layer.

Removing upper spring, the model is simplified to Winkler-Pasternak foundation (Pasternak, 1954):

$$F_f \equiv F_p = -K_w w_0 + K_s \frac{\partial^2 w_0}{\partial x^2} \quad (18)$$

where K_w and K_s are spring and shear stiffness coefficient, respectively.

Further simplification by removing shear layer leads to Winkler model of foundation:

$$F_f \equiv F_W = -K_w w_0 \quad (19)$$

Derived equations of motion for macro-scale FGM porous beam are expressed as:

$$\delta u_0: \frac{\partial N_{xx}}{\partial x} = I_0 \ddot{u}_0 + I_1 \ddot{\phi}_x - c_1 I_3 \left(\dot{\phi}_x + \frac{\partial \dot{w}_0}{\partial x} \right) \quad (20a)$$

$$\delta \varphi_x: \frac{\partial M_{xx}}{\partial x} - c_1 \frac{\partial P_{xx}}{\partial x} - N_{xz} + c_2 R_{xz} = I_1 \ddot{u}_0 + I_2 \ddot{\phi}_x - c_1 I_3 \ddot{u}_0 - c_1 I_4 \left(2\dot{\phi}_x + \frac{\partial \dot{w}_0}{\partial x} \right) + c_1^2 I_6 \left(\dot{\phi}_x + \frac{\partial \dot{w}_0}{\partial x} \right) \quad (20b)$$

$$\delta w_0: c_1 \frac{\partial^2 P_{xx}}{\partial x^2} + \frac{\partial N_{xz}}{\partial x} - c_2 \frac{\partial R_{xz}}{\partial x} - \hat{N}_{xx} \frac{\partial^2 w_0}{\partial x^2} + \left(\frac{K_l K_u}{K_l + K_u} \right) w_0 - \left(\frac{G K_u}{K_l + K_u} \right) \frac{\partial^2 w_0}{\partial x^2} = I_0 \ddot{w}_0 + c_1 I_3 \frac{\partial \ddot{u}_0}{\partial x} + c_1 I_4 \frac{\partial \ddot{\phi}_x}{\partial x} - c_1^2 I_6 \left(\frac{\partial \ddot{\phi}_x}{\partial x} + \frac{\partial^2 \ddot{w}_0}{\partial x^2} \right) \quad (20c)$$

Substituting particular form of constitutive equations (Eq. 8) into thickness-integrated forces and moments (Eq. 13) in order to obtain nonlocal forces and moments in final nonlocal forms:

$$(1 - \mathfrak{B}\nabla^2) N_{xx} = (1 - \ell^2 \nabla^2) \left[A_{xx}^{(0)} \frac{\partial u_0}{\partial x} + A_{xx}^{(1)} \frac{\partial \varphi_x}{\partial x} - c_1 A_{xx}^{(3)} \left(\frac{\partial \varphi_x}{\partial x} + \frac{\partial^2 w_0}{\partial x^2} \right) \right] \quad (21a)$$

$$(1 - \mathfrak{B}\nabla^2) M_{xx} = (1 - \ell^2 \nabla^2) \left[A_{xx}^{(1)} \frac{\partial u_0}{\partial x} + A_{xx}^{(2)} \frac{\partial \varphi_x}{\partial x} - c_1 A_{xx}^{(4)} \left(\frac{\partial \varphi_x}{\partial x} + \frac{\partial^2 w_0}{\partial x^2} \right) \right] \quad (21b)$$

$$(1 - \mathfrak{B}\nabla^2) P_{xx} = (1 - \ell^2 \nabla^2) \left[A_{xx}^{(3)} \frac{\partial u_0}{\partial x} + A_{xx}^{(4)} \frac{\partial \varphi_x}{\partial x} - c_1 A_{xx}^{(6)} \left(\frac{\partial \varphi_x}{\partial x} + \frac{\partial^2 w_0}{\partial x^2} \right) \right] \quad (21c)$$

$$(1 - \mathfrak{B}\nabla^2) N_{xz} = (1 - \ell^2 \nabla^2) \left[A_{xz}^{(0)} \left(\varphi_x + \frac{\partial w_0}{\partial x} \right) - c_2 A_{xz}^{(2)} \left(\varphi_x + \frac{\partial w_0}{\partial x} \right) \right] \quad (21d)$$

$$(1 - \mathfrak{B}\nabla^2) R_{xz} = (1 - \ell^2 \nabla^2) \left[A_{xz}^{(2)} \left(\varphi_x + \frac{\partial w_0}{\partial x} \right) - c_2 A_{xz}^{(4)} \left(\varphi_x + \frac{\partial w_0}{\partial x} \right) \right] \quad (21e)$$

where resultant stiffness coefficients are obtained as:

$$\left\{ A_{xx}^{(0)}, A_{xx}^{(1)}, A_{xx}^{(2)}, A_{xx}^{(3)}, A_{xx}^{(4)}, A_{xx}^{(6)} \right\} = b \int_{-h/2}^{h/2} C_{xx} \{1, z, z^2, z^3, z^4, z^6\} dz \quad (22a)$$

$$\left\{ A_{xz}^{(0)}, A_{xz}^{(2)}, A_{xz}^{(4)} \right\} = b \int_{-h/2}^{h/2} C_{xz} \{1, z^2, z^4\} dz \quad (22b)$$

Substituting nonlocal forces and moments (Eq. 21) into equations of motion (Eq. 19), three equations of motion of the nano-beam expressed by displacements are derived in the form:

$$A_{xx}^{(0)} \frac{\partial^2 u_0}{\partial x^2} + A_{xx}^{(1)} \frac{\partial^2 \varphi_x}{\partial x^2} - c_1 A_{xx}^{(3)} \left(\frac{\partial^2 \varphi_x}{\partial x^2} + \frac{\partial^3 w_0}{\partial x^3} \right) - \ell^2 \left[A_{xx}^{(0)} \frac{\partial^4 u_0}{\partial x^4} + A_{xx}^{(1)} \frac{\partial^4 \varphi_x}{\partial x^4} - c_1 A_{xx}^{(3)} \left(\frac{\partial^4 \varphi_x}{\partial x^4} + \frac{\partial^5 w_0}{\partial x^5} \right) \right] = I_0 \ddot{u}_0 + I_1 \ddot{\phi}_x - c_1 I_3 \left(\dot{\phi}_x + \frac{\partial \dot{w}_0}{\partial x} \right) - \mathfrak{B} \left[I_0 \frac{\partial^2 \ddot{u}_0}{\partial x^2} + I_1 \frac{\partial^2 \ddot{\phi}_x}{\partial x^2} - c_1 I_3 \left(\frac{\partial^2 \ddot{\phi}_x}{\partial x^2} + \frac{\partial^3 \ddot{w}_0}{\partial x^3} \right) \right] \quad (23a)$$

$$-A_{xz}^{(0)} \left(\varphi_x + \frac{\partial w_0}{\partial x} \right) + 2c_2 A_{xz}^{(2)} \left(\varphi_x + \frac{\partial w_0}{\partial x} \right) - c_2^2 A_{xz}^{(4)} \left(\varphi_x + \frac{\partial w_0}{\partial x} \right) + A_{xx}^{(1)} \frac{\partial^2 u_0}{\partial x^2} - c_1 A_{xx}^{(3)} \frac{\partial^2 u_0}{\partial x^2} + A_{xx}^{(2)} \frac{\partial^2 \varphi_x}{\partial x^2} - c_1 A_{xx}^{(4)} \frac{\partial^2 \varphi_x}{\partial x^2} - c_1 A_{xx}^{(4)} \left(\frac{\partial^2 \varphi_x}{\partial x^2} + \frac{\partial^3 w_0}{\partial x^3} \right) + c_1^2 A_{xx}^{(6)} \left(\frac{\partial^2 \varphi_x}{\partial x^2} + \frac{\partial^3 w_0}{\partial x^3} \right) - \ell^2 \left[-A_{xz}^{(0)} \left(\frac{\partial^2 \varphi_x}{\partial x^2} + \frac{\partial^3 w_0}{\partial x^3} \right) + 2c_2 A_{xz}^{(2)} \left(\frac{\partial^2 \varphi_x}{\partial x^2} + \frac{\partial^3 w_0}{\partial x^3} \right) - c_2^2 A_{xz}^{(4)} \left(\frac{\partial^2 \varphi_x}{\partial x^2} + \frac{\partial^3 w_0}{\partial x^3} \right) + A_{xx}^{(1)} \frac{\partial^4 u_0}{\partial x^4} - c_1 A_{xx}^{(3)} \frac{\partial^4 u_0}{\partial x^4} + A_{xx}^{(2)} \frac{\partial^4 \varphi_x}{\partial x^4} - c_1 A_{xx}^{(4)} \frac{\partial^4 \varphi_x}{\partial x^4} - c_1 A_{xx}^{(4)} \left(\frac{\partial^4 \varphi_x}{\partial x^4} + \frac{\partial^5 w_0}{\partial x^5} \right) + c_1^2 A_{xx}^{(6)} \left(\frac{\partial^4 \varphi_x}{\partial x^4} + \frac{\partial^5 w_0}{\partial x^5} \right) \right] = I_1 \ddot{u}_0 - c_1 I_3 \ddot{u}_0 + I_2 \ddot{\phi}_x + c_1^2 I_6 \left(\dot{\phi}_x + \frac{\partial \dot{w}_0}{\partial x} \right) - c_1 I_4 \left(2\dot{\phi}_x + \frac{\partial \dot{w}_0}{\partial x} \right) - \mathfrak{B} \left[I_1 \frac{\partial^2 \ddot{u}_0}{\partial x^2} - c_1 I_3 \frac{\partial^2 \ddot{u}_0}{\partial x^2} + I_2 \frac{\partial^2 \ddot{\phi}_x}{\partial x^2} + c_1^2 I_6 \left(\frac{\partial^2 \ddot{\phi}_x}{\partial x^2} + \frac{\partial^3 \ddot{w}_0}{\partial x^3} \right) - c_1 I_4 \left(2 \frac{\partial^2 \ddot{\phi}_x}{\partial x^2} + \frac{\partial^3 \ddot{w}_0}{\partial x^3} \right) \right] \quad (23b)$$

$$c_1 A_{xx}^{(3)} \frac{\partial^3 u_0}{\partial x^3} + A_{xz}^{(0)} \left(\frac{\partial \varphi_x}{\partial x} + \frac{\partial^2 w_0}{\partial x^2} \right) - 2c_2 A_{xz}^{(2)} \left(\frac{\partial \varphi_x}{\partial x} + \frac{\partial^2 w_0}{\partial x^2} \right) + c_2^2 A_{xz}^{(4)} \left(\frac{\partial \varphi_x}{\partial x} + \frac{\partial^2 w_0}{\partial x^2} \right) + c_1 A_{xx}^{(4)} \frac{\partial^3 \varphi_x}{\partial x^3} - c_1^2 A_{xx}^{(6)} \left(\frac{\partial^3 \varphi_x}{\partial x^3} + \frac{\partial^4 w_0}{\partial x^4} \right) - \ell^2 \left[c_1 A_{xx}^{(3)} \frac{\partial^5 u_0}{\partial x^5} + A_{xz}^{(0)} \left(\frac{\partial^3 \varphi_x}{\partial x^3} + \frac{\partial^4 w_0}{\partial x^4} \right) - 2c_2 A_{xz}^{(2)} \left(\frac{\partial^3 \varphi_x}{\partial x^3} + \frac{\partial^4 w_0}{\partial x^4} \right) + c_2^2 A_{xz}^{(4)} \left(\frac{\partial^3 \varphi_x}{\partial x^3} + \frac{\partial^4 w_0}{\partial x^4} \right) + c_1 A_{xx}^{(4)} \frac{\partial^5 \varphi_x}{\partial x^5} - c_1^2 A_{xx}^{(6)} \left(\frac{\partial^5 \varphi_x}{\partial x^5} + \frac{\partial^6 w_0}{\partial x^6} \right) \right] = I_0 \ddot{w}_0 + c_1 I_3 \frac{\partial \ddot{u}_0}{\partial x} + c_1 I_4 \frac{\partial \ddot{\phi}_x}{\partial x} - c_1^2 I_6 \left(\frac{\partial \ddot{\phi}_x}{\partial x} + \frac{\partial^2 \ddot{w}_0}{\partial x^2} \right) + \hat{N}_{xx} \frac{\partial^2 w_0}{\partial x^2} + \frac{K_l K_u}{K_l + K_u} w_0 - \frac{G K_u}{K_l + K_u} \frac{\partial^2 w_0}{\partial x^2} - \mathfrak{B} \left[I_0 \frac{\partial^2 \ddot{w}_0}{\partial x^2} + c_1 I_3 \frac{\partial^3 \ddot{u}_0}{\partial x^3} + c_1 I_4 \frac{\partial^3 \ddot{\phi}_x}{\partial x^3} - c_1^2 I_6 \left(\frac{\partial^3 \ddot{\phi}_x}{\partial x^3} + \frac{\partial^4 \ddot{w}_0}{\partial x^4} \right) + \hat{N}_{xx} \frac{\partial^4 w_0}{\partial x^4} + \frac{K_l K_u}{K_l + K_u} \frac{\partial^2 w_0}{\partial x^2} - \frac{G K_u}{K_l + K_u} \frac{\partial^4 w_0}{\partial x^4} \right] \quad (23c)$$

5. SOLUTION OF THE PROBLEM

Analytical solution for simply supported FGM porous nano-beam is derived using Navier solution technique. The generalized displacements are expanded in trigonometric series in form of:

$$\begin{pmatrix} u_0 \\ \varphi_x \\ w_0 \end{pmatrix} = \sum_{n=1}^{\infty} \begin{pmatrix} \bar{u} \cos(\beta_n x) e^{i\omega_n t} \\ \bar{\varphi} \cos(\beta_n x) e^{i\omega_n t} \\ \bar{w} \sin(\beta_n x) e^{i\omega_n t} \end{pmatrix} \wedge \beta_n = \frac{n\pi}{L} \quad (24)$$

where \bar{u} , $\bar{\varphi}$, \bar{w} are maximum values of displacements and ω_n is natural frequency of the n-th mode.

The system of three governing equations for free vibration analysis is defined as:

$$\{[K] - \omega_n^2 [M]\} \{\Delta\} = 0 \quad (25)$$

where $[K]$ and $[M]$ are stiffness and inertia matrices with size 3x3, and Δ are displacements in vector form:

$$\{\Delta\} = [\bar{u} \ \bar{\varphi} \ \bar{w}]^T \quad (26)$$

Stiffness and inertia matrices are symmetric ($K_{ij} = K_{ji}$, $M_{ij} = M_{ji}$). Coefficients of these matrices are obtained as:

$$K_{11} = -A_{xx}^{(0)} \beta_n^2 - \ell^2 A_{xx}^{(0)} \beta_n^4 \quad (27a)$$

$$K_{12} = -A_{xx}^{(1)} \beta_n^2 + c_1 A_{xx}^{(3)} \beta_n^2 + \ell^2 (-A_{xx}^{(1)} \beta_n^4 + c_1 A_{xx}^{(3)} \beta_n^4) \quad (27b)$$

$$K_{13} = c_1 A_{xx}^{(3)} \beta_n^3 + \ell^2 c_1 A_{xx}^{(3)} \beta_n^5 \quad (27c)$$

$$K_{22} = -A_{xz}^{(0)} + 2c_2A_{xz}^{(2)} - c_2^2A_{xz}^{(4)} - A_{xx}^{(2)}\beta_n^2 + 2c_1A_{xx}^{(4)}\beta_n^2 - c_1^2A_{xx}^{(6)}\beta_n^2 + \ell^2(-A_{xz}^{(0)}\beta_n^2 + 2c_2A_{xz}^{(2)}\beta_n^2 - c_2^2A_{xz}^{(4)}\beta_n^2 - A_{xx}^{(2)}\beta_n^4 + 2c_1A_{xx}^{(4)}\beta_n^4 - c_1^2A_{xx}^{(6)}\beta_n^4) \quad (27d)$$

$$K_{23} = -A_{xz}^{(0)}\beta_n + 2c_2A_{xz}^{(2)}\beta_n - c_2^2A_{xz}^{(4)}\beta_n + c_1A_{xx}^{(4)}\beta_n^3 - c_1^2A_{xx}^{(6)}\beta_n^3 + \ell^2(-A_{xz}^{(0)}\beta_n^3 + 2c_2A_{xz}^{(2)}\beta_n^3 - c_2^2A_{xz}^{(4)}\beta_n^3 + c_1A_{xx}^{(4)}\beta_n^5 - c_1^2A_{xx}^{(6)}\beta_n^5) \quad (27e)$$

$$K_{33} = -A_{xz}^{(0)}\beta_n^2 + 2c_2A_{xz}^{(2)}\beta_n^2 - c_2^2A_{xz}^{(4)}\beta_n^2 - c_1^2A_{xx}^{(6)}\beta_n^4 + \ell^2(-A_{xz}^{(0)}\beta_n^4 + 2c_2A_{xz}^{(2)}\beta_n^4 - c_2^2A_{xz}^{(4)}\beta_n^4 - c_1^2A_{xx}^{(6)}\beta_n^6) - \frac{K_lK_u}{K_l+K_u} - \frac{GK_u}{K_l+K_u}\beta_n^2 + \hat{N}_{xx}\beta_n^2 + \mathfrak{B}\left(\frac{K_lK_u}{K_l+K_u}\beta_n^2 - \frac{GK_u}{K_l+K_u}\beta_n^4 + \hat{N}_{xx}\beta_n^4\right) \quad (27f)$$

$$M_{11} = -I_0 - \mathfrak{B}I_0\beta_n^2 \quad (28a)$$

$$M_{12} = -I_1 + c_1I_3 + \mathfrak{B}(-I_1\beta_n^2 + c_1I_3\beta_n^2) \quad (28b)$$

$$M_{13} = c_1I_3\beta_n + \mathfrak{B}c_1I_3\beta_n^3 \quad (28c)$$

$$M_{22} = -I_2 + 2c_1I_4 - c_1^2I_6 + \mathfrak{B}(-I_2\beta_n^2 + 2c_1I_4\beta_n^2 - c_1^2I_6\beta_n^2) \quad (28d)$$

$$M_{23} = c_1I_4\beta_n - c_1^2I_6\beta_n + \mathfrak{B}(c_1I_4\beta_n^3 - c_1^2I_6\beta_n^3) \quad (28e)$$

$$M_{33} = -I_0 - c_1^2I_6\beta_n^2 + \mathfrak{B}(-I_0\beta_n^2 - c_1^2I_6\beta_n^4) \quad (28f)$$

6. RESULTS AND DISCUSSION

Free vibration analysis of FGM porous nanobeam with simply supported edges is conducted in the present section. Firstly, the comparison of obtained numerical results with results from the literature is shown to verify the correctness of the present model. Then, the free vibration analysis of functionally graded porous nanobeam is presented in the following subsection.

6.1. Verification

Eigenfrequencies for functionally graded beam are compared with results on the basis of sinusoidal shear deformation theory (Thai and Vo, 2012b) and presented in Table 1. The parameters $L = 10 m$, $\nu = 0.3$, $E_1 = 380 GPa$, $E_2 = 70 GPa$, $\rho_1 = 3960 kg/m^3$, $\rho_2 = 2702 kg/m^3$ were applied to obtain the results.

Tab. 1. Dimensionless natural frequency $\bar{\omega} = \sqrt{\omega} \sqrt[4]{\frac{L^4 \rho A}{EI_2}}$ of simply supported beam

L/h	g	Thai and Vo (2012b)	Present
5	0	5.1531	5.1528
	1	3.9907	3.9904
	2	3.6263	3.6264
20	5	3.3998	3.4012
	0	5.4603	5.4603
	1	4.2051	4.2051
	2	3.8361	3.8361
	5	3.6485	3.6485

Table 2 presents the comparison of calculated first three modes of free vibrations with results obtained based on sinusoidal shear deformation theory and nonlocal strain gradient theory (Lu et al., 2017). The following parameters were used to obtain the numerical results: $L = 10 nm$, $L/h = 10$, $\nu = 0.3$, $E = 30 MPa$, $\rho = 1 kg/m^3$.

Tab. 2. First three modes of dimensionless natural frequency

$$\bar{\omega}_n = \omega_n L^2 \sqrt[4]{\frac{I_0}{EI_2}} \text{ of simply supported nanobeam}$$

ω_n	\mathfrak{B}	ℓ/h	Lu et al. (2017)	Present	
ω_1	0	0	9.7077	9.7075	
			9.2614	9.2612	
			8.2198	8.2197	
	0.5	0	9.8267	9.8266	
			9.3750	9.3748	
			8.3206	8.3205	
	1	1	10.1755	10.1753	
			9.7077	9.7075	
			8.6159	8.6158	
	ω_2	0	0	37.1009	37.0981
				31.4146	31.4122
				23.1019	23.1001
0.5		0	38.8887	38.8857	
			32.9283	32.9258	
			24.2151	24.2133	
1		1	43.8165	43.8132	
			37.1009	37.0981	
			27.2835	27.2815	
ω_3		0	0	78.1855	78.1719
				56.8977	56.8878
				36.6416	36.6353
	0.5	0	86.4318	86.4168	
			62.8988	62.8879	
			40.5062	40.4992	
	1	1	107.4379	107.4190	
			78.1855	78.1719	
			50.3508	50.3420	

Tab. 3. Dimensionless natural frequency $\bar{\omega} = \sqrt{\omega} \sqrt[4]{\frac{L^4 \rho A}{EI_2}}$ of simply supported beam

\bar{K}_w	$\frac{\bar{K}_s}{\pi^2}$	Karami and Janghorban (2019)	Present
0	0	3.216341	3.216341
	0.5	3.532519	3.532519
	1	3.781208	3.781208
	2.5	4.326928	4.326928
10^2	0	3.793132	3.793132
	0.5	3.998874	3.998874
	1	4.177015	4.177015
	2.5	4.607107	4.607107
10^4	0	10.02651	10.02651
	0.5	10.03856	10.03856
	1	10.05058	10.05058
	2.5	10.08636	10.08636

Table 3 contains the comparison of fundamental frequency of homogeneous macro-sized beam resting on Winkler-Pasternak foundation (Karami and Janghorban, 2019). We have not found any numerical results in tabular form for nanobeam resting on Kerr foundation. Winkler-Pasternak stiffness coefficients are dimensionless, and takes the form: $\bar{K}_w = K_w \frac{L^4}{EI_2}$, $\bar{K}_s = K_s \frac{L^2}{EI_2}$. Numerical results are obtained for the following parameters: $L = 10 \text{ m}$, $L/h = 120$, $\nu = 0.3$, $E = 30 \text{ MPa}$, $\rho = 1 \text{ kg/m}^3$, $C_{xx} = \frac{E(z)}{1-\nu^2}$.

It can be concluded, from Tables 1–3 that the numerical results from the present model are in good agreement with the results from the previous papers.

6.2. Free vibration analysis

In the present subsection, free vibrations analysis is conducted for simply supported FGM nanobeam with diverse porosity distributions. In the study, geometrical and material properties are assumed as constant: length $L = 50 \text{ nm}$, constant thickness $h = 10 \text{ nm}$ and unit width b . Young's moduli take values $E_t = 380 \text{ GPa}$, $E_b = 70 \text{ GPa}$, densities $\rho_t = 3100 \text{ kg/m}^3$, $\rho_b = 2700 \text{ kg/m}^3$ and constant Poisson's ratio $\nu = 0.3$. During investigation, the power-law index is assumed to be constant $g = 2$.

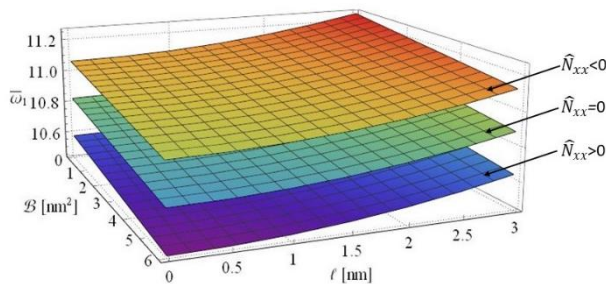


Fig. 4. Effect of nonlocal parameter \mathfrak{B} and length scale parameter l in conjunction with compressive/tensile forces on dimensionless fundamental frequencies of FGM nanobeam

Figure 4 presents the influence of nonlocal parameters \mathfrak{B} , l on dimensionless fundamental frequencies ($\bar{\omega}_1 = 10^2 \cdot \omega_1 L^2 \sqrt{I_0/E_t I_2}$) of FGM nanobeam without porosity. The figure shows softening (increasing nonlocal parameter \mathfrak{B}) and hardening (increasing length scale parameter l) effects according to Eringen's nonlocal theory and Mindlin's strain gradient theory, respectively. The figure also shows the dependence of axial in-plane compressive ($\bar{N}_{xx} > 0$) and tensile ($\bar{N}_{xx} < 0$) forces on dimensionless natural frequencies. Applied compressive forces cause weakening of the structure stiffness, in consequence, its eigenfrequencies decrease. Opposite phenomenon may be observed for tensile force. Nanobeam stiffness increases, thus its fundamental frequencies increase. The phenomena are similar to situations observed by Timoshenko and Woinowsky-Krieger (1959) in bending of rectangular plates subjected to compressive/tensile axial in-plane forces.

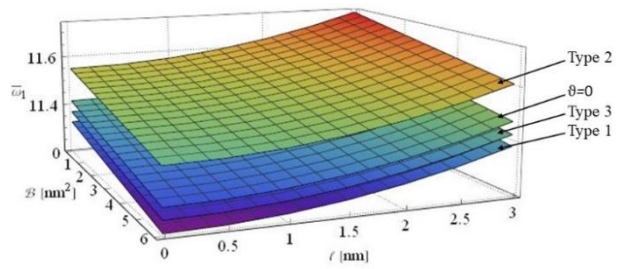


Fig. 5. Effect of nonlocal parameter \mathfrak{B} and length scale parameter l in conjunction with diverse porosity types on dimensionless fundamental frequencies of FGM nanobeam under tensile forces

Natural frequencies for FGM nanobeam subjected to tensile forces without porosity and with diverse porosity types (with porosity coefficient $\theta = 0.3$) are presented in Figure 5. Based on the material properties' variation (Fig. 3) and porosity distribution (Fig. 2), it can be observed that porosity Type 1 and Type 3 have similar influence on the response of structure. Porosity causes the structures to become lighter and softer, and consequently, dimensionless fundamental frequencies decrease for Type 1 and Type 3. Ratio of mass to stiffness of FGM nanobeam for Type 2 (porosity accumulated at the bottom surface with lower value of Young's modulus) is higher than for structure without porosity, therefore, fundamental frequencies are also higher.

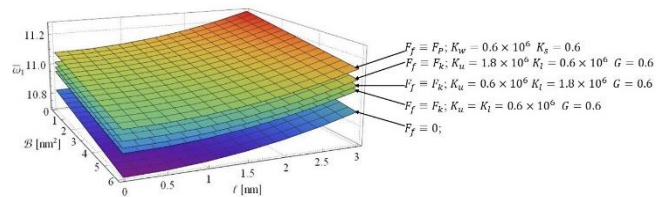


Fig. 6. Effect of nonlocal parameter \mathfrak{B} and length scale parameter l in conjunction with reaction of foundation on dimensionless fundamental frequencies of FGM nanobeam

Figure 6 shows the comparison of Winkler-Pasternak and Kerr foundations effects on eigenfrequencies of FGM nanobeam without porosity. It is clearly observed that the foundation effect causes the whole vibrational system to become stiffer, and thus, natural frequencies increase. Fundamental frequencies of nanobeam resting on Kerr foundation are lower in comparison to Winkler-Pasternak foundation with the same springs and shear moduli stiffnesses. Nevertheless, Kerr foundation, due to more parameters, gives an opportunity to more precisely control the dynamic behavior of the nanobeam.

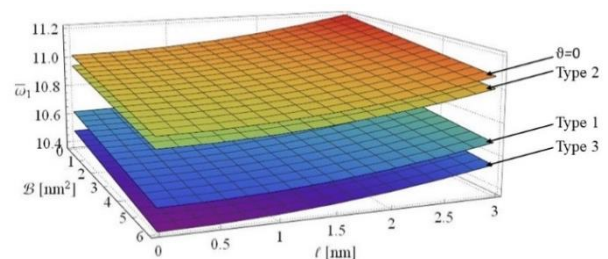


Fig. 7. Effect of nonlocal parameter \mathfrak{B} and length scale parameter l in conjunction with diverse porosity types on dimensionless fundamental frequencies of FGM nanobeam resting on Kerr foundation

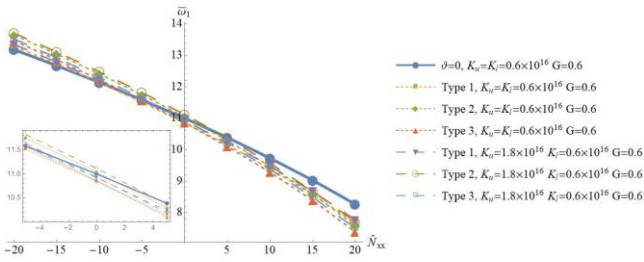


Fig. 8. Effect of axial in-plane forces in conjunction with diverse porosity types on dimensionless fundamental frequencies of FGM nanobeam resting on Kerr foundation.

Dependence of eigenfrequencies of nanobeam resting on Kerr foundation on various porosity types (porosity coefficient $\vartheta = 0.6$) is presented in Figure 7. Similar to previous analysis, porosity Type 1 and Type 3 have a similar impact on natural frequencies. From the figure, it can be also observed that increas-

ing porosity coefficient value causes decreasing of resultant stiffness for porosity distribution Type 2, and natural frequencies are lower for structure without porosity (compare with Fig. 5).

Figure 8 presents the effect of compressive/tensile forces of FGM nanobeam with various porosity distribution and foundation stiffness. It may be observed that natural frequencies of the nanobeam decrease with increasing compressive force. It is related to the weakening of nanobeam stiffness under compressive force. Opposite effect, increasing structural stiffness, occur with increasing tensile forces. Therefore, increase of tensile forces' value causes an increase of nanobeams eigenfrequencies.

Numerical results for natural frequencies of FGM nanobeam resting on Kerr foundation with diverse porosity distribution and subjected to compressive/tensile forces are presented in Table 4. Following results are calculated for nonlocal parameters $\mathfrak{B} = 2$ and $\ell = 2$.

Tab. 4. Dimensionless natural frequency ($\bar{\omega}_1 = 10^2 \cdot \omega_1 L^2 \sqrt{\frac{I_0}{E_t I_2}}$) of elastically supported FGM porous nanobeam under axial in-plane forces

\hat{N}_{xx}	G	K_u [· 10 ¹⁶]	K_l [· 10 ¹⁶]	Type 1,2,3	Type 1	Type 2	Type 3
				ϑ			
				0		0.3	
-10	0	0	0	12.0200	11.9992	12.2672	12.0856
				12.1355	12.1284	12.4052	12.2236
	0.6	0.6	1.8	12.1605	12.1563	12.4349	12.2533
			1.8	12.1929	12.1926	12.4736	12.2920
	1.2	0.6	1.8	12.2993	12.3114	12.6004	12.4187
			1.8	12.1680	12.1648	12.4439	12.2623
		1.8	0.6	12.1767	12.1744	12.4543	12.2727
			1.8	12.2414	12.2467	12.5314	12.3498
-5	0	0	0	11.4592	11.3695	11.5941	11.4123
				11.5803	11.5059	11.7400	11.5583
	0.6	0.6	1.8	11.6065	11.5353	11.7715	11.5897
			1.8	11.6404	11.5735	11.8123	11.6306
	1.2	0.6	1.8	11.7519	11.6986	11.9461	11.7645
			1.8	11.6144	11.5442	11.7810	11.5993
		1.8	0.6	11.6235	11.5544	11.7919	11.6102
			1.8	11.6912	11.6305	11.8733	11.6917
0	0	0	0	10.8694	10.7029	10.8795	10.6966
				10.9971	10.8476	11.0348	10.8522
	0.6	0.6	1.8	11.0246	10.8788	11.0683	10.8857
			1.8	11.0604	10.9193	11.1117	10.9292
	1.2	0.6	1.8	11.1776	11.0519	11.2539	11.0716
			1.8	11.0330	10.8882	11.0784	10.8959
		1.8	0.6	11.0425	10.8990	11.0900	10.9075
			1.8	11.1138	10.9797	11.1766	10.9942
5	0	0	0	10.2458	9.9918	10.1144	9.9294
				10.3811	10.1467	10.2813	10.0969
	0.6	0.6	1.8	10.4103	10.1800	10.3172	10.1328
			1.8	10.4481	10.2232	10.3638	10.1796
	1.2	0.6	1.8	10.5722	10.3648	10.5161	10.3323
			1.8	10.4191	10.1901	10.3281	10.1438

			1.8	10.4292	10.2016	10.3405	10.1562
	1.8	0.6	10.5047	10.2878	10.4333	10.2493	
		1.8	10.6095	10.4073	10.5618	10.3782	
	0	0	9.5816	9.2259	9.2864	9.0976	
		0.6	9.7262	9.3935	9.4680	9.2802	
	0.6	1.8	9.7573	9.4294	9.5069	9.3193	
		1.8	9.7977	9.4762	9.5575	9.3701	
10		1.8	9.9298	9.6287	9.7224	9.5358	
		0.6	9.7667	9.4404	9.5187	9.3312	
	1.2	1.8	9.7775	9.4528	9.5322	9.3447	
		0.6	9.8580	9.5458	9.6328	9.4458	
		1.8	9.9695	9.6744	9.7719	9.5855	

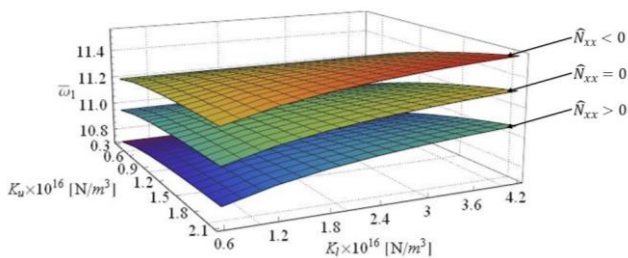


Fig. 9. Effect of Kerr foundation in conjunction with compressive/tensile forces on dimensionless fundamental frequencies of FGM nanobeam

It is observed from Figure 9 that natural frequencies of FGM nanobeam increase with increasing stiffness of both springs of Kerr foundation because the whole system becomes stiffer. For this analysis, the stiffness value of shear layer is assumed to be constant $G = 0.6$. Foundation response does not change the dynamical behavior of the structure under tensile ($\bar{N}_{xx} < 0$) and compressive ($\bar{N}_{xx} > 0$) forces. Nanobeam subjected to tensile/compressive forces undergoes increasing/decreasing of stiffness, consequently eigen frequencies increase/decrease.

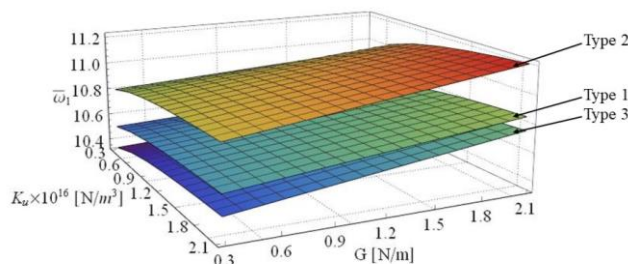


Fig. 10. Effect of Kerr foundation in conjunction with diverse porosity distribution on dimensionless fundamental frequencies of FGM nanobeam.

Figure 10 illustrates the influence of Kerr foundation on the dimensionless fundamental frequency of the nanobeam for diverse porosity distribution. For every considered porosity distribution, natural frequencies increase with increasing both stiffness coefficient of the foundation. For this analysis, stiffness value of lower spring is assumed to be constant $K_1 = 0.6$. Influence of

elastic foundation does not change the free vibration characteristic for the investigated porosity distributions.

7. CONCLUSIONS

In the present paper, comprehensive analysis of free vibration is conducted for the generalized model of FGM nanobeam with diverse porosity distribution, axial in-plane forces and elastic foundation. The nanobeam is modelled using the nonlocal strain gradient-based Reddy higher-order shear deformation theory. Equations of motion have been derived on the basis of the dynamical version of Hamilton principle and the analytical solution for free vibration problems of simply supported nanobeam is obtained in closed-form using Navier solution technique. Present results have been compared with the results from the literature. The parametric analysis examined the effect of axial in-plane forces, porosity distribution, and foundation response in conjunction with both nonlocal parameters on dynamical behavior of simply supported nanobeam.

The present study and the obtained results may be applied to validate different analytical and numerical methods to analyze nanostructures. Additionally, the numerical results can be used in the analysis and optimization of FGM porous nanostructures in NEMS devices.

REFERENCES

1. Ashoori A.R, Salari E., Sadough Vanini S.A., (2017), A Thermo-Electro-Mechanical Vibration Analysis of Size-Dependent Functionally Graded Piezoelectric Nanobeams, *Advances in High Temperature Ceramic Matrix Composites and Materials for Sustainable Development; Ceramic Transactions*, Vol. 263, 547–558.
2. Aydogdu M., (2009), A general nonlocal beam theory: Its application to nanobeam bending, buckling and vibration, *Physica E: Low-dimensional Systems and Nanostructures*, Vol. 41(9), 1651–1655.
3. Bhushan B. (Ed), (2004), *Springer Handbook of Nanotechnology*, Springer Verlag, Berlin.
4. El-Borgi S., Fernandes R., Reddy J.N., (2015), Non-local free and forced vibrations of graded nanobeams resting on a non-linear elastic foundation, *International Journal of Non-Linear Mechanics*, Vol. 77, 348–363.
5. Eltahir M.A., Emam S.A., Mahmoud F.F., (2012), Free vibration analysis of functionally graded size-dependent nanobeams. *Applied Mathematics and Computation*, Vol. 218(14), 7406–7420.

6. **Eltaher M.A., Emam S.A., Mahmoud F.F.**, (2013), Static and stability analysis of nonlocal functionally graded nanobeams, *Composite Structures*, Vol. 96, 82–88.
7. **Eltaher M.A., Fouda N., El-midany, T., Sadoun, A.M.**, (2018), Modified porosity model in analysis of functionally graded porous nanobeams. *Journal of the Brazilian Society of Mechanical Sciences and Engineering*, Vol. 40, 141.
8. **Eringen A.C.**, (1972), Nonlocal polar elastic continua. *International Journal of Engineering Science*, Vol. 10(1), 1–16.
9. **Eringen A.C., Edelen D.G.B.**, (1972), On nonlocal elasticity. *International Journal of Engineering Science*, Vol. 10(3), 233–248.
10. **Ghadiri M., Rajabpour A., Akbarshahi A.**, (2017), Non-linear forced vibration analysis of nanobeams subjected to moving concentrated load resting on a viscoelastic foundation considering thermal and surface effects, *Applied Mathematical Modelling*, Vol. 50, 676–694.
11. **Karami B., Janghorban M.**, (2019), A new size-dependent shear deformation theory for free vibration analysis of functionally graded/anisotropic nanobeams, *Thin-Walled Structures*, Vol. 143, 106227.
12. **Kerr A.D.**, (1965), A study of a new foundation model. *Acta Mechanica*, Vol. 1(2), 135–147.
13. **Kim J., Żur K.K., Reddy, J.N.**, (2019), Bending, free vibration, and buckling of modified couples stress-based functionally graded porous micro-plates, *Composite Structures*, Vol. 209, 879–888.
14. **Lam D.C.C., Yang F., Chong A.C.M., Wang J., Tong P.**, (2003), Experiments and theory in strain gradient elasticity, *Journal of the Mechanics and Physics of Solids*, Vol. 51(8), 1477–1508.
15. **Leondes C.T. (Ed)**, (2006), *MEMS/NEMS Handbook Techniques and Applications*, Springer, New York.
16. **Li L., Hu Y.**, (2015), Buckling analysis of size-dependent nonlinear beams based on a nonlocal strain gradient theory, *International Journal of Engineering Science*, Vol. 97, 84–94.
17. **Lim C.W., Li C., Yu J.-L.**, (2010), Free vibration of pre-tensioned nanobeams based on nonlocal stress theory, *Journal of Zhejiang University-SCIENCE A*, Vol. 11, 34–42.
18. **Lim C.W., Zhang G., Reddy J.N.**, (2015), A higher-order nonlocal elasticity and strain gradient theory and its applications in wave propagation. *Journal of the Mechanics and Physics of Solids*, Vol. 78, 298–313.
19. **Lu L., Guo X., Zhao J.**, (2017), Size-dependent vibration analysis of nanobeams based on the nonlocal strain gradient theory, *International Journal of Engineering Science*, Vol. 116, 12–24.
20. **Lv Z., Qiu Z., Zhu J., Zhu B., Yang W.**, (2018), Nonlinear free vibration analysis of defective FG nanobeams embedded in elastic medium, *Composite Structures*, Vol. 202, 675–685.
21. **Lyshevski S.E.**, (2002), *MEMS and NEMS: System, Devices and Structures*, CRC Press, New York.
22. **Mindlin R.D.**, (1964), Micro-structure in linear elasticity. *Archive for Rational Mechanics and Analysis*, Vol. 16, 51–78.
23. **Mindlin R.D.**, (1965), Second gradient of strain and surface-tension in linear elasticity. *International Journal of Solids and Structures* Vol. 1(4), 417–438.
24. **Nazemnezhad R., Hosseini-Hashemi S.**, (2014), Nonlocal nonlinear free vibration of functionally graded nanobeams, *Composite Structures*, Vol. 110, 192–199.
25. **Pasternak P.L.**, (1954), *On a New method of Analysis of an Elastic Foundation by Means of Two Foundation Constants*, Gosudarstvennoe Izdatelstvo Literaturi po Stroitelstvu I Arkhitekture, Moscow.
26. **Rahmani O., Jandaghian A.A.**, (2015), Buckling analysis of functionally graded nanobeams based on a nonlocal third-order shear deformation theory. *Applied Physics A*, Vol. 119, 1019–1032.
27. **Reddy J.N.**, (2017), *Energy principles and variational methods in applied mechanics*, John Wiley & Sons, New York.
28. **Reza Barati M.**, (2017), Investigating dynamic response of porous inhomogeneous nanobeams on hybrid Kerr foundation under hygro-thermal loading, *Applied Physics A*, Vol. 123, 332.
29. **Saffari S., Hashemian M., Toghraie D.**, (2017), Dynamic stability of functionally graded nanobeam based on nonlocal Timoshenko theory considering surface effects, *Physica B: Condensed Matter*, Vol. 520, 97–105.
30. **Sahmani S., Ansari R.**, (2011), Nonlocal beam models for buckling of nanobeams using state-space method regarding different boundary conditions, *Journal of Mechanical Science and Technology*, Vol. 25, 2365.
31. **Shafiei N., Mirjavadi S.S., Afshari B.M., Rabby S., Kazemi, M.**, (2017), Vibration of two-dimensional imperfect functionally graded (2D-FG) porous nano-/micro-beams, *Computer Methods in Applied Mechanics and Engineering*, Vol. 322, 615–632.
32. **Şimşek M.**, (2014), Large amplitude free vibration of nanobeams with various boundary conditions based on the nonlocal elasticity theory, *Composites Part B: Engineering*, Vol. 56, 621–628.
33. **Şimşek M.**, (2016), Nonlinear free vibration of a functionally graded nanobeam using nonlocal strain gradient theory and a novel Hamiltonian approach, *International Journal of Engineering Science*, Vol. 105, 12–27.
34. **Thai H.T.**, (2012), A nonlocal beam theory for bending, buckling, and vibration of nanobeams, *International Journal of Engineering Science*, Vol. 52, 56–64.
35. **Thai H.T., Vo T.P.**, (2012a), A nonlocal sinusoidal shear deformation beam theory with application to bending, buckling, and vibration of nanobeams. *International Journal of Engineering Science*, Vol. 54, 58–66.
36. **Thai H.T., Vo, T.P.**, (2012b), Bending and free vibration of functionally graded beams using various higher order shear deformation beam theories. *International Journal of Mechanical Sciences*, Vol. 62(1), 57–66.
37. **Timoshenko S., Woinowsky-Krieger S.**, (1959), *Theory of plates and shells*, McGraw-Hill Book Company, New York.
38. **Toupin R.A.**, (1962), Elastic materials with couple-stresses. *Archive for Rational Mechanics and Analysis*, Vol. 11, 385–414.
39. **Yang F., Chong A.C.M., Lam D.C.C., Tong P.**, (2002), Couple stress based strain gradient theory for elasticity, *International Journal of Solids and Structures*, Vol. 39(10), 2731–2743.
40. **Zhang K, Ge M.-H., Zhao C., Deng Z.-C., Lu, X.-J.**, (2019), Free vibration of nonlocal Timoshenko beams made of functionally graded materials by Symplectic method, *Composites Part B: Engineering*, 156, 174–184.

The work has been conducted within W/WM-IIM/3/2020 project and was financed by the funds of the Ministry of Science and Higher Education, Poland.